Applied Physics Letters

Temperature-dependent resistivity of alternative metal thin films

Cite as: Appl. Phys. Lett. **117**, 043104 (2020); https://doi.org/10.1063/5.0015048
Submitted: 23 May 2020 . Accepted: 15 July 2020 . Published Online: 29 July 2020

Marco Siniscalchi, Davide Tierno, Kristof Moors, Zsolt Tőkei, and Christoph Adelmann

View Online Export Citation CrossMark

ARTICLES YOU MAY BE INTERESTED IN

Spin orientation and strain tuning valley polarization with magneto-optic Kerr effects in ferrovalley VS_2 monolayer
Applied Physics Letters **117**, 042406 (2020); https://doi.org/10.1063/5.0006474

An insight into the charge carriers transport properties and electric field distribution of $CH_3NH_3PbBr_3$ thick single crystals
Applied Physics Letters **117**, 041904 (2020); https://doi.org/10.1063/5.0011713

Scanning magneto-optical Kerr effect (MOKE) measurement with element-selectivity by using a soft x-ray free-electron laser and an ellipsoidal mirror
Applied Physics Letters **117**, 042405 (2020); https://doi.org/10.1063/5.0012348

Lock-in Amplifiers up to 600 MHz
Watch

AIP Publishing

© 2020 Author(s).

Applied Physics Letters ARTICLE scitation.org/journal/apl

Temperature-dependent resistivity of alternative metal thin films

Cite as: Appl. Phys. Lett. **117**, 043104 (2020); doi: 10.1063/5.0015048
Submitted: 23 May 2020 · Accepted: 15 July 2020 ·
Published Online: 29 July 2020

View Online Export Citation CrossMark

Marco Siniscalchi,[1,2,a] Davide Tierno,[1] Kristof Moors,[3] Zsolt Tőkei,[1] and Christoph Adelmann[1,b]

AFFILIATIONS

[1]Imec, 3001 Leuven, Belgium
[2]Politecnico di Milano, Dipartimento di Chimica, Materiali e Ingegneria Chimica "Giulio Natta," 20131 Milano, Italy
[3]Forschungszentrum Jülich, Peter Grünberg Institut, 52428 Jülich, Germany

[a]**Present address:** Department of Materials, University of Oxford, Oxford, United Kingdom.
[b]**Author to whom correspondence should be addressed:** christoph.adelmann@imec.be

ABSTRACT

The temperature coefficients of the resistivity (TCR) of Cu, Ru, Co, Ir, and W thin films have been investigated as a function of film thickness below 10 nm. Ru, Co, and Ir show bulk-like TCR values that are rather independent of the thickness, whereas the TCR of Cu increases strongly with the decreasing thickness. Thin W films show negative TCR values, which can be linked to high disorder. The results are qualitatively consistent with a temperature-dependent semiclassical thin-film resistivity model that takes into account phonon, surface, and grain boundary scattering. The results indicate that the thin-film resistivity of Ru, Co, and Ir is dominated by grain boundary scattering, whereas that of Cu is strongly influenced by surface scattering.

Published under license by AIP Publishing. https://doi.org/10.1063/5.0015048

The perennial scaling of complementary metal-oxide-semiconductor (CMOS) circuits requires the equal miniaturization of the interconnect wires that link individual transistors.[1–3] Today, interconnect dimensions have reached about 15 nm and are expected to reduce below 10 nm in the near future. At such small dimensions, the currently used Cu metallization suffers from a strongly increased resistance due to finite size effects of the resistivity[4] and scaling limitations of the barriers and liners required to ensure the interconnect reliability.[5,6] As a result, the overall performance of CMOS circuits is increasingly limited by the interconnect.[7] This has prompted much research to find alternative metals that could replace Cu with both improved reliability and resistivity at small dimensions. Recently, this has led to the introduction of Co in local interconnects.[8]

Although Cu has a lower bulk resistivity than the proposed alternative metals, it has been argued[7,9,10] and later experimentally observed[11,12] that metals with a shorter mean free path of the charge carriers can outperform Cu in thin films or narrow wires due to a reduced sensitivity to surface and grain boundary scattering. However, there is still no consensus on the relative importance of the various scattering contributions and their material dependence. The understanding of the relative importance of scattering mechanisms is crucial for the optimization of the interconnect resistance, and thus, a simple and robust measurement methodology is desirable. Typically, surface and grain boundary scattering has been modeled as a function of film thickness and grain size within semiclassical approaches,[13–16] but the disentanglement of the different scattering contributions is not straightforward since the resulting thickness dependences are rather similar and Matthiessen's rule does not apply.[12,16] Temperature-dependent resistivity measurements have been proposed as a possible improvement[17–19] since semiclassical models describe the thin-film resistivity by the ratio of film thickness or grain size to the mean free path of the bulk metal. The mean free path varies with temperature, and therefore, temperature-dependent resistivity measurements can be used to test the applicability and consistency of semiclassical models and their parameters beyond the description of the simple thickness dependence of the resistivity. Moreover, it has been shown that temperature-dependent resistivity measurements are capable of distinguishing qualitatively between dominant surface and grain boundary scattering. Concretely, dominant surface scattering typically leads to a stronger temperature dependence of the resistivity, whereas grain boundary scattering leaves it unaffected.[19] However, only a few temperature-dependent thin-film resistivity measurements have been reported on a limited set of materials, and the experimental results have not been yet systematically compared to semiclassical models.[20–24] Hence, no consistent picture has emerged yet.

Published under license by AIP Publishing

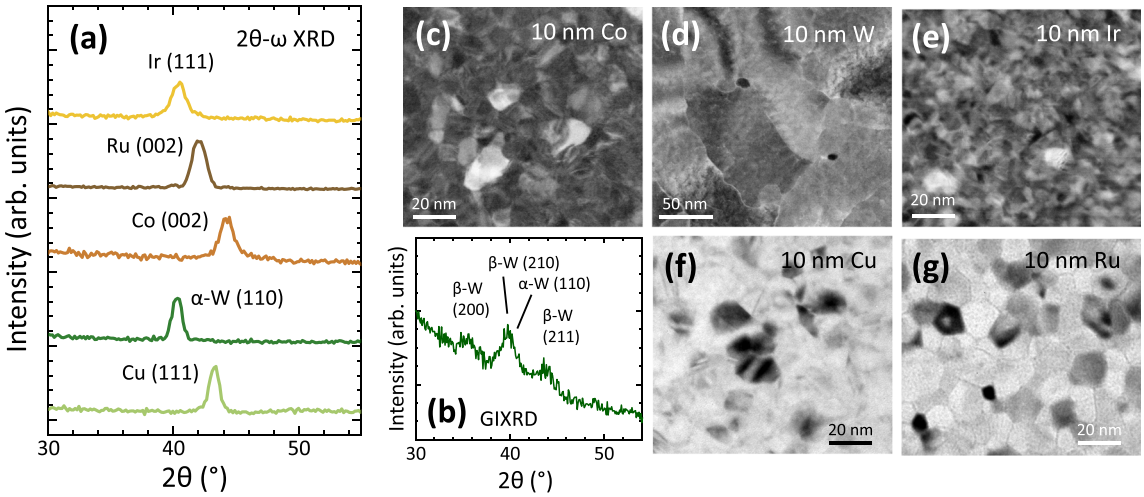

FIG. 1. (a) 2θ–ω x-ray diffraction pattern of the studied 10 nm thick metal films, as indicated. (b) Grazing-incidence x-ray diffraction pattern of the 3 nm thick W film. Plan-view dark-field scanning transmission electron micrographs of 10 nm thick (c) Co, (d) W, and (e) Ir films. (f) and (g) show plan-view bright-field transmission electron micrographs of 10 nm thick Cu and Ru films, respectively.

Here, we report on the temperature coefficients of the resistivity (TCR) of Cu, Ru, Co, Ir, and W films with thicknesses between 3 and 10 nm. The experimentally measured linear TCR values at room temperature are compared with the results of a temperature-dependent semiclassical model for thin-film resistivities. Good qualitative agreement between experiment and model was observed although the magnitude of the observed variation was different for Cu. This demonstrates both the relevance and the quantitative limitations of semiclassical models to describe thin-film resistivities.

All films were deposited by physical vapor deposition (PVD) in a Canon Anelva EC7800 system at room temperature on 300 mm Si (100) wafers. Prior to metal deposition, a 100 nm-thick thermal SiO_2 was grown to ensure electrical isolation. Ru, Ir, and W were directly deposited on SiO_2, whereas Co and Cu were sandwiched between 1.5 nm thick TaN layers *in situ* to avoid oxidation in air. The parallel conductance of the TaN layers was negligible. Film thicknesses were determined by a combination of x-ray reflectivity and Rutherford backscattering spectrometry. X-ray diffraction [XRD, 2θ–ω geometry, Cu Kα radiation, Fig. 1(a)] indicated that the films were polycrystalline with strong (111), (110), and (001) texture for the fcc (Cu, Ir), bcc (W), and hcp (Co, Ru) metals, respectively. For W, the appearance of the β-W phase was observed for the thinnest films by grazing-incidence x-ray diffraction [GIXRD, $\omega = 0.3°$, Cu Kα radiation, Fig. 1(b)]. The rms surface roughness measured by atomic force microscopy was 3–5 Å for all films (not shown). Linear intercept lengths between grain boundaries were determined from plan-view transmission electron micrographs [Figs. 1(b)–1(f)].[12] Thin-film resistivities were obtained using both patterned Hall bars and sheet resistance measurements. The TCR was obtained from the Hall bar resistivity at temperatures between 25 °C and 125 °C. In the studied temperature window, the resistivity was found to increase linearly with temperature within experimental precision, *i.e.,* the TCR was approximately constant.

Figure 2 shows the measured resistivities of the different metal thin films at room temperature as a function of their thickness. For all cases, the resistivity increased with the decreasing thickness due to increasing contributions of surface and grain boundary scattering in thinner films. For thicknesses of 5 nm and above, Cu had clearly the lowest resistivity. However, for 3 nm thick films, resistivities of alternative metals (except W) became comparable, consistent with previous reports.[12] This has been explained by the longer mean free path of Cu with respect to the other metals,[10] which renders Cu much more sensitivity to finite size effects. Figure 3 shows the experimentally determined TCR of the same set of thin films as a function of their thickness. The TCR of Cu was close to the bulk value of $6.6 \times 10^{-3}\,\mu\Omega$ cm[25] for the thickest film but increased strongly as the film thickness decreased. For 3 nm thick Cu, the TCR was about 70% higher than the bulk value. TCR values for Ru, Ir, and Co films were close to bulk values[25] for thicknesses between 10 and 5 nm, with some reduction below the bulk value for the thinnest Ru

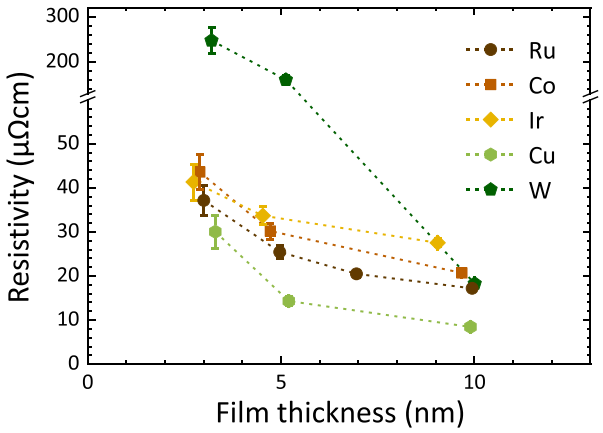

FIG. 2. Experimental room-temperature resistivities of the studied thin films as a function of their thickness.

Published under license by AIP Publishing

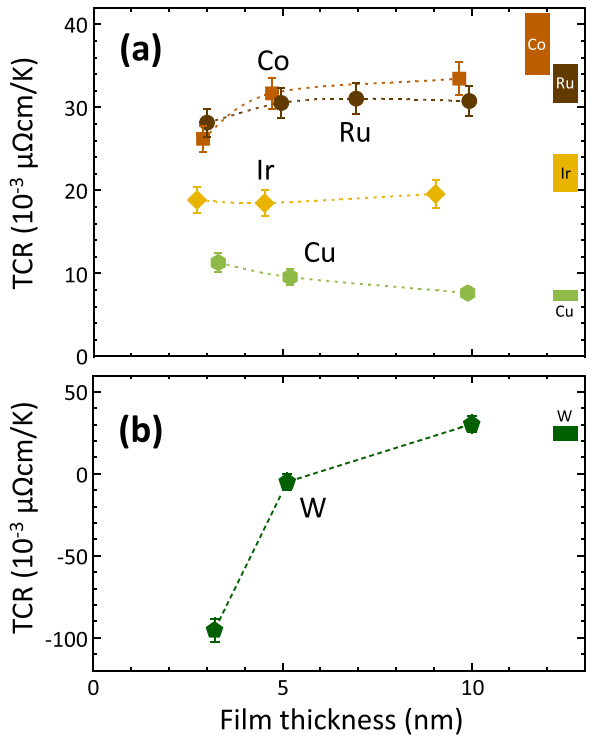

FIG. 3. Experimental TCR values near room temperature of the studied thin films as a function of their thickness. The boxes on the right hand side of the graphs indicate the range of bulk TCR values in Ref. 25.

(by about 10%) and Co (by about 20%) films. For Ir, this decrease was absent and even the thinnest film showed a bulk-like TCR within experimental accuracy. By contrast, the behavior of W was distinctly different [Fig. 3(b)]. While the TCR was close to the bulk value for the 10 nm thick film, it decreased sharply with the decreasing thickness to a strongly negative value at a film thickness of 3 nm.

To shed light on the experimental observations, the temperature dependence of the thin-film resistivity was calculated using a semiclassical model based on the work of Mayadas and Shatzkes (MS).[16,19,26] In the MS model, the thickness dependence of the resistivity in the presence of surface and grain boundary scattering is given by

$$\rho_{MS} = \left\{ \frac{1}{\rho_{GB}} - \frac{6}{\pi k \rho_0}(1-p)\int_0^{\pi/2} d\varphi \int_1^{\infty} dt \, \frac{\cos^2\varphi}{H^2(\varphi,t)} \times \left(\frac{1}{t^3} - \frac{1}{t^5}\right) \frac{1 - e^{-ktH(\varphi,t)}}{1 - pe^{-ktH(\varphi,t)}} \right\}^{-1}, \quad (1)$$

with the abbreviations $\rho_{GB} = \rho_0[1 - 3\alpha/2 + 3\alpha^2 - 3\alpha^3 \ln(1+1/\alpha)]^{-1}$, $\alpha = \frac{\lambda_0}{g}\frac{2R}{1-R}$, and $H(\varphi,t) = 1 + \alpha/\cos\varphi\sqrt{(1-1/t^2)}$. Here, ρ_0 is the bulk resistivity of the metal, h is the film thickness, λ is the mean free path of the charge carriers, $k = h/\lambda$, and g is the mean linear intercept length between grain boundaries. $0 \le R \le 1$ is the grain boundary reflection coefficient and determines the strength of grain boundary scattering. The parameter p describes the scattering at the surfaces or interfaces of the films with a value of 0 corresponding to fully diffuse and 1 to fully specular scattering.

The MS model does not depend explicitly on the temperature T, but implicitly via the bulk mean free path $\lambda(T)$ and the bulk resistivity $\rho_0(T)$. It has, however, been shown that the product $\rho_0 \times \lambda \equiv A$ is a function of the Fermi surface morphology only and can be calculated by *ab initio* methods.[10,12] Moreover, the product A is independent of temperature for $T \ll T_F$, with T_F being the Fermi temperature of the metal. The temperature dependence of the bulk resistivity $\rho_0(T)$ in the presence of phonon and (weak) impurity scattering can be described by the Bloch–Grüneisen model,

$$\rho_0(T) = \rho_{\text{imp}} + CT^5 \int_0^{\Theta_D/T} \frac{x^5}{(e^x - 1)(1 - e^{-x})} dx, \quad (2)$$

where ρ_{imp} describes the residual (temperature-independent) resistivity due to impurity or point defect scattering. Θ_D is the Debye temperature, and C is a prefactor that can be determined from the bulk room-temperature resistivity. In high-purity PVD films, impurity scattering can be neglected at room temperature. The temperature dependence of the mean free path $\lambda(T)$ can then be calculated by $\lambda(T) = A/\rho_0(T)$. This is equivalent to assuming that the carrier density in the metal is independent of temperature and the temperature dependence of the resistivity is determined by scattering only, which is generally well obeyed in metals. Equation (2) then allows for the calculation of $\lambda(T)$, which, in turn, can be used to calculate the temperature-dependent thin-film resistivity using Eq. (1).[26] An analytical model of the TCR based on this approach has been published by Marom and Eizenberg.[19] However, it is straightforward to calculate the temperature-dependent resistivity numerically using Eq. (1) and to obtain the TCR by differentiation. The materials parameters used for the calculation of the TCR of the different metal films are listed in Table I.

In general, the calculated TCR decreased weakly (by about 2%) between 300 K and 400 K, which is below experimental precision, and therefore, the TCR at 300 K is reported for simplicity. Values for the different metals are shown as a function of film thickness in Fig. 4. For Co, Ru, and Ir, the calculated TCR values were independent of thickness (less than 5% variation) and within 3% of the calculated bulk value, in good agreement with the experimental results. This indicates that the increase in the thin-film resistivity with the decreasing thickness is independent of temperature. Such a behavior has been linked to cases where the thin-film resistivity is dominated by grain boundary scattering.[19,26] The results for Ru confirm a previous analysis of the

TABLE I. Material parameters used for modeling the TCR: room-temperature bulk resistivity $\rho_{0,\text{rt}}$, room-temperature mean free path $\lambda_{0,\text{rt}}$, temperature-independent $\rho_0 \times \lambda_0$ product,[10,12] Debye temperature Θ_D,[27] grain boundary scattering parameter R, and surface scattering parameter p.[2,4,12,23,28]

	$\rho_{0,\text{rt}}$ ($\mu\Omega$ cm)	$\lambda_{0,\text{rt}}$ (nm)	$\rho_0 \times \lambda_0$ ($10^{-16}\Omega$ m^2)	Θ_D (K)	R	p
Cu	1.7	39.9	6.70	320	0.22	0
Co	6.2	7.8	4.82	365	0.37	0
Ru	7.8	6.6	5.14	385	0.50	1
Ir	5.2	7.1	3.69	285	0.50	1
W	5.3	15.5	8.20	320	0.55	0

Published under license by AIP Publishing

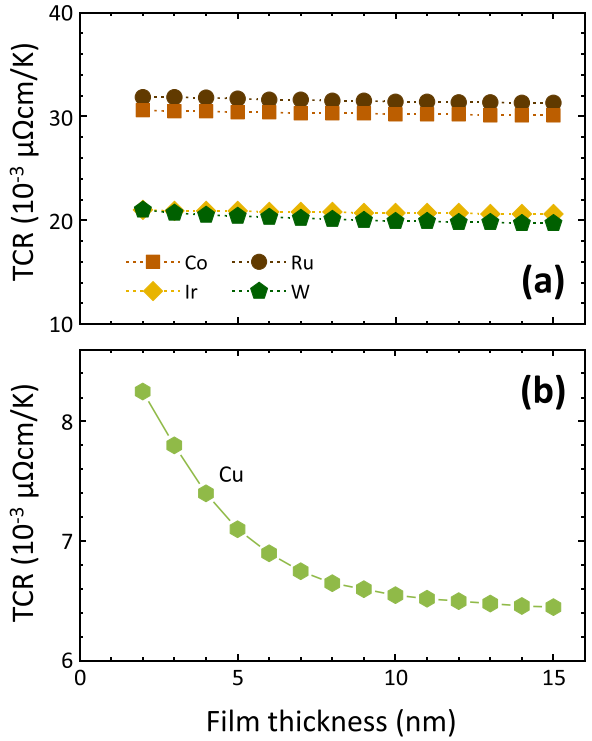

FIG. 4. Calculated film thickness dependence of the TCR at 300 K for (a) Co, Ir, Ru, and W and (b) Cu.

thickness dependence of the Ru thin-film resistivity,[12] indicating the dominance of grain boundary scattering. Similar to scattering by point defects, quantum-mechanical tunneling through grain boundaries is expected to depend only very weakly on temperature, which is consistent with both the modeled and experimentally observed behavior.

In addition, the increase in the experimental TCR of a 3 nm thick Cu film by about 70% over the bulk could also be qualitatively explained within the semiclassical model. In this model, an increasing TCR for the decreasing film thickness has been found in cases of strong contributions of surface scattering to the thin-film resistivity.[19,26] This confirms a previous analysis of the thickness dependence of the Cu thin-film resistivity.[12] However, the measured increase in the thin-film TCR with respect to the bulk value was about three times as large as the calculated one. This suggests that the above semiclassical model only describes qualitative aspects of the resistivity of thin metallic films in the presence of surface scattering. Such limitations may stem from various sources, such as the assumption of an isotropic free electron gas or from the omission of point defect scattering and quantum confinement effects in the semiclassical model. These results may also qualitatively explain a previous report, which found that the thickness dependence of the Cu thin-film resistivity required different fitting parameters p and R at different temperatures.[21] While it cannot be ruled out that p and R depend indeed on temperature, our findings suggest that the discrepancies may at least partially stem from limitations of the model to accurately and consistently describe thin-film resistivities at different temperatures. The results also suggest that temperature-dependent measurements are well suited to test the accuracy of future improved models of thin-film or nanowire resistivity.

By contrast, the negative TCR for W [Fig. 3(b)] cannot be explained within the semiclassical model for metallic thin films described above. The semiclassical model predicts that the W thin-film resistivity increases weakly with the decreasing thickness, which stems from a nonnegligible influence of surface scattering due to the relatively long mean free path of W [Fig. 4(a)]. Lower-than-bulk and even negative TCR values have, however, been observed for highly resistive metals, especially with resistivities around or above the Ioffe–Regel limit.[29–31] The behavior has been attributed to localization effects due to large disorder and a breakdown of Matthiessen's rule between point defect or grain boundary scattering and phonon scattering.[29–32] Charge carrier localization leads generally to a weaker temperature dependence of the resistivity. Thermal activation effects when localization energies become comparable to the thermal energy can even lead to negative TCR values. Moreover, in the case of strong disorder, contributions of impurity or grain boundary scattering and phonon scattering are not an addition anymore and cannot be clearly separated. Since both the semiclassical MS model in Eq. (1) and the Bloch–Grüneisen model in Eq. (2) explicitly assume the validity of Matthiessen's rule between phonon and grain boundary or impurity scattering,[16] such effects cannot be described within the above approach.

For W, the large disorder for the thinnest films may be linked to the appearance of the high-resistivity β-W phase, as demonstrated in Fig. 1(b). The formation of β-W has been typically observed for PVD films below a certain critical thickness, typically between 5 and 20 nm,[33,34] depending on the deposition conditions. We note that such negative TCR values were not observed for W deposited by chemical vapor deposition.[35]

The same disorder and localization effects leading to the breakdown of Matthiessen's rule between point defect or grain boundary scattering and phonon scattering may also explain the observed reduction of the TCR of the thinnest Ru and Co films. Films deposited by PVD often contain a disordered nanocrystalline interface layer at the substrate due to random nucleation, limited adatom mobility, and/or high stress. The disorder in such ultrathin nanocrystalline may be not only due to point defects but also due to a high density of grain boundaries. All these effects can lead to (weak) localization of the charge carriers close to the interface and the observed reduction of the TCR.

In conclusion, we have studied the TCR of Cu, Co, Ru, Ir, and W thin films with thicknesses between 3 and 10 nm. The TCR of Co, Ru, and Ir was bulk-like except for the thinnest films, where the TCR was slightly reduced. By contrast, the TCR of Cu increased with the decreasing thickness and became larger than the bulk value. These observations could be qualitatively explained by a semiclassical model for the temperature dependence of the thin-film resistivity. In agreement with a previous analysis of the thickness dependence of the thin-film resistivity,[12] the model was consistent with the predominance of grain boundary scattering in Co, Ru, and Ir, whereas the behavior of Cu was influenced by a strong contribution of surface scattering. By contrast, the TCR of W became strongly negative for the thinnest films, indicating the presence of strong disorder, presumably due to the appearance of the high-resistivity β-W phase.

Published under license by AIP Publishing

The results indicate that semiclasssical thin-film resistivity models[16] can describe the TCR qualitatively without the need for assuming temperature-dependent model parameters. However, the models fail to describe the measured thickness- and temperature-dependence quantitatively in a consistent way for predominant surface scattering. This hints toward limitations of such semiclassical models to describe the resistivity of thin metallic films in all cases fully quantitatively. Improved models, e.g., taking the band structure into account, may thus be required for a quantitative consistent picture of the thin-film resistivity and its thickness and temperature dependence.

This work was supported by imec's industrial affiliation program on nano-interconnects. M.S. acknowledges co-funding by the Erasmus+ program of the European Union. The authors would like to thank Sofie Mertens and Thomas Witters (imec) for the support of the PVD depositions as well as imec's Materials and Components Analysis (MCA) Laboratory for the electron micrographs, the atomic force microscopy, and the Rutherford backscattering measurements.

DATA AVAILABILITY

The data that support the findings of this study are available from the corresponding author upon reasonable request.

REFERENCES

[1]J. D. Meindl, Comp. Sci. Eng. **5**, 20 (2003).
[2]J. S. Clarke, C. George, C. Jezewski, A. Maestre Caro, D. Michalak, and J. Torres, in IEEE Symposium VLSI Technology-Technical Digest (2014) Vol. 1.
[3]M. R. Baklanov, C. Adelmann, L. Zhao, and S. de Gendt, ECS J. Solid State Sci. Technol. **4**, Y1 (2015).
[4]D. Josell, S. H. Brongersma, and Z. Tőkei, Annu. Rev. Mater. Res. **39**, 231 (2009).
[5]K. Croes, C. Wu, D. Kocaay, Y. Li, P. Roussel, J. Bömmels, and Z. Tőkei, ECS J. Solid State Sci. Technol. **4**, N3094 (2015).
[6]A. S. Oates, ECS J. Solid State Sci. Technol. **4**, N3168 (2015).
[7]P. Kapur, J. P. McVittie, and K. C. Saraswat, IEEE Trans. Electron Devices **49**, 590 (2002).
[8]C. Auth, A. Aliyarukunju, M. Asoro, D. Bergstrom, V. Bhagwat, J. Birdsall, N. Bisnik, M. Buehler, V. Chikarmane, G. Ding, Q. Fu, H. Gomez, W. Han, D. Hanken, M. Haran, M. Hattendorf, R. Heussner, H. Hiramatsu, B. Ho, S. Jaloviar, I. Jin, S. Joshi, S. Kirby, S. Kosaraju, H. Kothari, G. Leatherman, K. Lee, J. Leib, A. Madhavan, K. Marla, H. Meyer, T. Mule, C. Parker, S. Parthasarathy, C. Pelto, L. Pipes, I. Post, M. Prince, A. Rahman, S. Rajamani, A. Saha, J. D. Santos, M. Sharma, V. Sharma, J. Shin, P. Sinha, P. Smith, M. Sprinkle, A. St. Amour, C. Staus, R. Suri, D. Towner, A. Tripathi, A. Tura, C. Ward, and A. Yeoh, in Technical Digest-IEEE International Electron Device Meeting (2017), p. 29.1.1.
[9]C. Pan and A. Naeemi, IEEE Electron Device Lett. **35**, 250 (2014).
[10]D. Gall, J. Appl. Phys. **119**, 085101 (2016).
[11]L. G. Wen, P. Roussel, O. Varela Pedreira, B. Briggs, B. Groven, S. Dutta, M. I. Popovici, N. Heylen, I. Ciofi, K. Vanstreels, F. W. Østerberg, O. Hansen, D. H. Petersen, K. Opsomer, C. Detavernier, C. J. Wilson, S. Van Elshocht, K. Croes, J. Bömmels, Z. Tőkei, and C. Adelmann, ACS Appl. Mater. Interfaces **8**, 26119 (2016).
[12]S. Dutta, K. Sankaran, K. Moors, G. Pourtois, S. Van Elshocht, J. Bömmels, W. Vandervorst, Z. Tőkei, and C. Adelmann, J. Appl. Phys. **122**, 025107 (2017).
[13]K. Fuchs, Math. Proc. Cambridge Philos. Soc. **34**, 100 (1938).
[14]E. H. Sondheimer, Adv. Phys. **1**, 1 (1952).
[15]S. B. Soffer, J. Appl. Phys. **38**, 1710 (1967).
[16]A. F. Mayadas and M. Shatzkes, Phys. Rev. B **1**, 1382 (1970).
[17]P. M. T. M. van Attekum, P. H. Woerlee, G. C. Verkade, and A. A. M. Hoeben, Phys. Rev. B **29**, 645 (1984).
[18]J. W. C. De Vries, Thin Solid Films **167**, 25 (1988).
[19]H. Marom and M. Eizenberg, J. Appl. Phys. **96**, 3319 (2004).
[20]G. Kästle, H.-G. Boyen, A. Schröder, A. Plettl, and P. Ziemann, Phys. Rev. B **70**, 165414 (2004).
[21]J. J. Plombon, E. Andideh, V. M. Dubin, and J. Maiz, Appl. Phys. Lett. **89**, 113124 (2006).
[22]Q. G. Zhang, B. Y. Cao, X. Zhang, M. Fujii, and K. Takahashi, Phys. Rev. B **74**, 134109 (2006).
[23]D. Choi, X. Liu, P. K. Schelling, K. R. Coffey, and K. Barmak, J. Appl. Phys. **115**, 104308 (2014).
[24]Z. Cheng, Z. Xu, S. Xu, and X. Wang, J. Appl. Phys. **117**, 024307 (2015).
[25]J. Bass, in *Electrical Resistivity, Kondo and Spin Fluctuation Systems, Spin Glasses and Thermopower, Landolt-Brnstein—Group III Condensed Matter*, edited by K. H. Hellwege and J. L. Olsen (Springer, Berlin, Heidelberg, 1983), Vol. 15a, pp. 5–13.
[26]C. Adelmann, Solid-State Electron. **152**, 72 (2019).
[27]G. Grimvall, *Thermophysical Properties of Materials* (North Holland, Amsterdam, 1999).
[28]S. Dutta, S. Beyne, A. Gupta, S. Kundu, S. Van Elshocht, H. Bender, G. Jamieson, W. Vandervorst, J. Bömmels, C. J. Wilson, Z. Tőkei, and C. Adelmann, IEEE Electron Device Lett. **39**, 731 (2018).
[29]J. H. Mooij, Phys. Status Solidi A **17**, 521 (1973).
[30]Y. Imry, Phys. Rev. Lett. **44**, 469 (1980).
[31]C. C. Tsuei, Phys. Rev. Lett. **57**, 1943 (1986).
[32]S. Ciuchi, D. Di Sante, V. Dobrosavljević, and S. Fratini, npj Quantum Mater. **3**, 44 (2018).
[33]D. Choi, B. Wang, S. Chung, X. Liu, A. Darbal, A. Wise, N. T. Nuhfer, K. Barmak, A. P. Warren, K. R. Coffey, and M. F. Toney, J. Vac. Sci. Technol., A **29**, 051512 (2011).
[34]Q. Hao, W. Chen, and G. Xiao, Appl. Phys. Lett. **106**, 182403 (2015).
[35]E. Milosevic, V. Kamineni, X. Zhang, H. Dixit, M. V. Raymond, H. Huang, R. Southwick, C. Janicki, N. Lanzillo, and D. Gall, in Proceedings of the IEEE International Interconnect Technology Conference (IITC) (2018), Vol. 36.

Published under license by AIP Publishing